Synthesis, Structure, and Fluxional Behavior of Bis(cyclooctatetraene)ruthenium(0) and Its Derivatives

Martin A. Bennett,* Horst Neumann, and Anthony C. Willis

Research School of Chemistry, Australian National University, G.P.O. Box 414, Canberra, ACT 2601, Australia

Valter Ballantini and Paolo Pertici

Centro di Studio del CNR per le Macromolecole Stereordinate ed Otticamente Attive, Dipartimento di Chimica & Chimica Industriale, University of Pisa, via Risorgimento 35, 56100 Pisa, Italy

Brian E. Mann

Department of Chemistry, The University of Sheffield, Sheffield S3 7HF, England

Received January 29, 1997[⊗]

The complex Ru((1−6-η)-C_8H_8)((1−4-η)-C_8H_8) (**2**), which is made in two steps from Ru(acac)$_3$, shows three fluxional processes: (1) equilibration of the protons and carbon atoms of the (1−4-η)-C_8H_8 ring, which appear as a singlet even at −100 °C; (2) role reversal (exchange of hapticity) of the two rings; (3) a 1,5-shift within the (1−6-η)-C_8H_8 ring. Processes 2 and 3 cause the ^{1}H and ^{13}C resonances of C_8H_8 to appear as a broad singlet at room temperature, though the (1−6-η)-ring is static at *ca.* −60 °C. The free energies of activation $\Delta G^{\ddagger}_{235}$ for processes 2 and 3 have been estimated from magnetization transfer experiments to be 12.8 ± 0.2 and 13.5 ± 0.2 kcal mol^{-1}, respectively. Complex **2** reacts with ligands L to give adducts Ru(L)((1−4-η)-C_8H_8)((1,2,5,6-η)-C_8H_8) (L = CO (**4**), CN-*t*-Bu (**5**), P(OMe)$_3$ (**6**), PMe$_3$ (**7**), and PEt$_3$ (**8**)). The (1,2,5,6-η)-rings in these compounds are static at room temperature and do not exchange with the fluxional (1−4-η)-C_8H_8 rings. The (1−4-η)-C_8H_8 ring in **4** undergoes the usual 1,2-shift, the free energy of activation $\Delta G^{\ddagger}_{259}$ of 13.7 ± 0.1 kcal mol^{-1} being considerably higher than that of **2** or of Ru(CO)$_3$((1−4-η)-C_8H_8). The X-ray structures of **2**, **4**, **5**, and **7** are reported.

Introduction

Cyclooctatetraene (COT, C_8H_8)[1] forms numerous complexes, both mononuclear and polynuclear, with the d- and f-block elements, in which it displays a variety of bonding modes depending, in part, on the number of π-electrons that it contributes.[2,3] The fluxional behavior of COT complexes, especially of the metal tricarbonyls M(CO)$_3$((1−4-η)-C_8H_8) (M = Fe, Ru, Os) and M(CO)$_3$((1−6-η)-C_8H_8) (M = Cr, Mo, W), has played an important role in the study of nonrigidity in organometallic molecules.[4,5] In the case of iron, a bis(cyclooctatetraene) complex, Fe((1−6-η)-C_8H_8)((1−4-η)-C_8H_8) (**1**), has been isolated by reduction of $FeCl_3$ or Fe(acac)$_3$ in the presence of COT with an excess of isopropylmagnesium bromide[6,7] or, better, triethylaluminum.[8,9] Although the hapticity of the COT rings in **1** has been confirmed by single-crystal X-ray structural analysis,[10,11] in solution at room temperature the compound shows just a singlet in its ^{1}H and ^{13}C NMR spectra, indicating that the rings are equivalent on the NMR time scale. On cooling to −84 °C, a limiting spectrum is observed for the η^6-ring but the resonance for the η^4-ring remains a sharp singlet.[12,13] Complex **1** also catalyzes a variety of oligomerization reactions of alkenes and alkynes.[6,7,14] In view of the current interest in the organometallic chemistry and catalytic properties of zero valent ruthenium complexes containing arenes and polyenes as the only ligands, such as Ru((1−6-η)-1,3,5-C_8H_{10})(η^4-1,5-C_8H_{12})[15−17] and Ru(η^6-$C_{10}H_8$)(η^4-1,5-C_8H_{12}),[18,19] it is surprising that the ruthenium analogue of **1** is appar-

[⊗] Abstract published in *Advance ACS Abstracts,* May 15, 1997.

(1) Abbreviations and formulas: acac = acetylacetonate, 2,4-pentanedionato, $C_5H_7O_2$; COT = cyclooctatetraene, C_8H_8; COD = 1,5-cyclooctadiene, C_8H_{12}; NBD = norbornadiene (2,5-bicyclo[2.2.1]-heptadiene), C_7H_8; 1,3,5-C_8H_{10} = 1,3,5-cyclooctatriene; C_4H_6 = 1,3-butadiene.

(2) Fray, G. I.; Saxton, R. G. *The Chemistry of Cyclooctatetraene and its Derivatives*; Cambridge University Press: Cambridge, 1978; p 48.
(3) Deganello, G. *Transition Metal Complexes of Cyclic Polyolefins*; Academic: New York, 1979; Chapter 2.
(4) Cotton, F. A. In *Dynamic Nuclear Magnetic Resonance Spectroscopy*; Jackman, L. M., Cotton, F. A., Eds.; Academic: New York, 1975; Chapter 10, p 377.
(5) (a) Mann, B. E. In *Comprehensive Organometallic Chemistry*; Wilkinson, G., Stone, F. G. A., Abel, E. W., Eds.; Pergamon: Oxford, 1982; Vol. 3, p 89. (b) Mann, B. E. *Chem. Soc. Rev.* **1986**, *15*, 167.
(6) Carbonaro, A.; Greco, A.; Dall'Asta, G. *Tetrahedron Lett.* **1967**, 2037.
(7) Carbonaro, A.; Greco, A.; Dall'Asta, G. *J. Organomet. Chem.* **1969**, *20*, 177.
(8) Gerlach, D. H.; Peet, W. G.; Muetterties, E. L. *J. Am. Chem. Soc.* **1972**, *94*, 4545.
(9) Gerlach, D. H.; Schunn, R. A. *Inorg. Synth.* **1974**, *15*, 2.
(10) Allegra, G.; Colombo, A.; Immirzi, A.; Bassi, I. W. *J. Am. Chem. Soc.* **1968**, *90*, 4458.
(11) Allegra, G.; Colombo, A.; Mognaschi, E. R. *Gazz. Chim. Ital.* **1972**, *102*, 1060.
(12) Carbonaro, A.; Segre, A. L.; Greco, A.; Tosi, C.; Dall'Asta, G. *J. Am. Chem. Soc.* **1968**, *90*, 4453.
(13) Mann, B. E. *J. Chem. Soc., Dalton Trans.* **1978**, 1761.
(14) Carbonaro, A.; Greco, A.; Dall'Asta, G. *J. Org. Chem.* **1968**, *33*, 3948.
(15) Pertici, P.; Vitulli, G. *Comm. Inorg. Chem.* **1991**, *11*, 175.
(16) Mitsudo, T-A.; Hori, Y.; Watanabe, Y. *J. Organomet. Chem.* **1987**, *334*, 157.

S0276-7333(97)00065-4 CCC: $14.00

ently unknown. We describe here the synthesis of Ru((1−6-η)-C_8H_8)((1−4-η)-C_8H_8) (**2**) and some of its derivatives, together with a study of their fluxional behavior.

Experimental Section

All operations were carried out under purified nitrogen or argon with the use of standard Schlenk techniques. This is especially important in the handling of K_2[COT] and **2**. Before use, hydrocarbon and ether solvents were distilled from sodium benzophenone ketyl and CH_2Cl_2 was distilled from CaH_2. Cyclooctatetraene (COT) was stored at 0 °C and freshly distilled. Tris(acetylacetonato)ruthenium(III), $Ru(acac)_3$, was made in 70−80% yield from hydrated $RuCl_3$ and acetylacetone by published procedures or slight modifications thereof.[20−22]

The following instruments were used for NMR spectroscopic measurements: Varian Gemini 200 (^{1}H at 200.01 MHz; ^{13}C at 50.29 MHz), Gemini 300 (^{1}H at 300.10 MHz, ^{13}C at 75.43 MHz), VXR300S (^{1}H at 300.10 MHz, ^{13}C at 75.43 MHz), XL200E (^{31}P at 80.98 MHz) (Canberra), and Bruker WH400 (^{1}H at 400.13 MHz, ^{13}C at 100.62 MHz) (Sheffield). The temperature was measured with a Comark electronic thermometer, the sample being replaced with an NMR tube containing a thermocouple in CH_2Cl_2. The chemical shifts (δ) for ^{1}H and ^{13}C were referenced to residual solvent signals; those for ^{31}P are reported relative to external 85% H_3PO_4. Other instruments used were Perkin Elmer PE683 and 1800 for IR measurements and VG Micromass 7070F, Autospec, and ZAB-SEQ4 for the EI mass spectra at (70 eV). Elemental analyses were performed in the Microanalytical Unit of the Research School of Chemistry (Canberra).

The DANTE magnetization transfer measurements[23] were carried out as follows. A suitable temperature was chosen so that there was a little line broadening due to exchange. After the spectrometer had stabilized at that temperature, the probe was retuned, the T_1 values of the ^{13}CO groups were estimated using the $10D_1-\pi-D_1-\pi/2$ pulse sequence, adjusting the delay, D_1, for null signal. Subsequently, the relaxation delay was taken as $10D_1$. The DANTE pulse length was optimized for maximum signal inversion. The measurement was carried out using the pulse sequence {[read FID−{$10D_1-(D_2-P_1)_{30}-D_3-\pi/2$−acquire}$_8$−write FID−change D_3]$_m$−resetD_3}$_n$, with m = 8 and n chosen to give an adequate signal-to-noise. For Ru((1−6-η)-C_8H_8)((1−4-η)-C_8H_8)(**2**), D_1 = 1 s, D_2 = 0.2 ms, and P_1 = 1.0 μs for D_3 values of 3 μs, 0.04, 0.08, 0.16, 0.32, 0.64, 1.0, and 10.0s. The T_1 (average value) was determined as 2.2 s. For Ru(CO)((1−4-η)-C_8H_8)((1,2,5,6-η)-C_8H_8)(**4**), D_1 = 1.2 s, D_2 = 0.1 ms, and P_1 = 1.0 μs for D_3 values of 3 μs, 0.01, 0.02, 0.04, 0.08, 0.16, 0.32, 0.64, 1.0, and 10.0 s. Two interleaved sets of measurements were performed using a DANTE pulse at δ 56.2 for one set and δ 116.9 for the other. The T_1 (average value) was determined as 2.0 s.

X-ray Crystallography. Crystal data and details of data collection, data processing, structure analysis, and structure refinement are in Table 1. Lattice parameters were determined by least-squares analysis of the setting angles of 25 reflections 36.0° < 2θ < 45.0° for **2**, 41.2° < 2θ < 44.2° for **4**, 41.1° < 2θ < 47.0° for **5**, and 46.8° < 2θ < 50.2° for **7** (λ(Mo Kα_1) = 0.709 32 Å). All non-hydrogen atoms were refined anisotropically. For **2**, hydrogen atoms were placed at calculated positions (r(C−H) = 0.95 Å); these parameters were not refined in the crystallographic least-squares procedure but were periodically recalculated. For **4**, **5**, and **7**, the hydrogen atoms of C_8H_8 were observed in difference electron-density maps and included in the refinement; their coordinates were refined but their isotropic B-values were fixed.

In the case of **2**, examination of the electron density revealed a peak situated too close to other atoms of the structure to be a solvent atom, yet having no apparent chemical significance. Its coordinates were related to those of Ru(1) by the transformation (x, y, $^1/_2 + z$), suggestive of a stacking fault in the z direction. As a consequence, reflections with l-even and reflections with l-odd were put on separate scales, which were refined independently in the least-squares procedure. Disorder in the *tert*-butyl group of **5** was modeled by assuming two orientations of relative occupancies 0.57 and 0.43, and bond distances and angles within each orientation were restrained in the least-squares refinement.

Preparations. Bis(acetylacetonato)(cyclooctatetraene)-ruthenium(II), Ru(acac)$_2$((1,2,5,6-η)-C_8H_8) (3). A solution containing $Ru(acac)_3$ (4.0 g, 10 mmol) in THF (100 mL) was treated with freshly distilled COT (15 mL), a drop of water, and an excess of zinc amalgam, and the mixture was heated under reflux for 3 h. It was allowed to come to room temperature and filtered through Celite, and the orange-yellow filtrate was evaporated to dryness to give a sticky, red-brown residue. This was redissolved in ether, and the solution was dried overnight ($MgSO_4$). The solid remaining after removal of the solvent was recrystallized either from ether/hexane or ether to give orange-brown microcrystals of **3**, which were dried in vacuo at 60 °C. More **3** could be obtained in the form of a fine yellow powder by evaporation of the supernatant liquid. The yield of **3**, mp 126−128 °C, was 96−99%. ^{1}H NMR (C_6D_6): δ 1.73 (s), 2.07 (s, acac CH_3), 4.40 (dd), 4.82 (dd, J = 8.5, 2.5 Hz, coordinated =CH), 5.19 (s, acac CH), 6.11 (dd), 6.31 (dd) (J = 8.4, 2.5 Hz, uncoordinated =CH). ^{13}C{^{1}H} NMR (C_6D_6): δ 27.1, 28.4 (acac CH_3), 92.2 (acac CH), 96.6, 98.4 (coordinated C=C), 135.5, 136.3 (uncoordinated C=C). EI-MS (70 eV): m/z 400 (M), 300 (M − COT). IR (KBr, cm^{-1}): 1580 (vs), 1515 (vs), 1400 (vs, C=O, C=C stretch of acac). Anal. Calcd for $C_{18}H_{22}O_4Ru$: C, 53.59; H, 5.50. Found: C, 53.65; H, 5.47.

Bis(cyclooctatetraene)ruthenium(0), Ru((1−6-η)-C_8H_8)-((1−4-η)-C_8H_8) (2). A suspension of potassium sand (800 mg, 20.6 mmol) in THF (60 mL) contained in a 250 mL two-necked Schlenk flask was cooled to 0 °C, and freshly distilled COT (1.5 mL, 13.3 mmol) was added from a syringe. The mixture was stirred at 0 °C for 4 h and evaporated to dryness in vacuo. Ether (60 mL) was added, and the suspension was again evaporated to dryness. The yellow-brown solid residue (CAUTION: flammable in air) was again treated with ether (60 mL), the suspension was cooled in dry ice/acetone, and an ice-cold solution of **3** (900 mg, 2.23 mmol) in ether (60 mL) was added. The mixture was stirred overnight, the cooling bath being kept at −40 °C. The resulting orange suspension was evaporated to *ca.* half the volume under reduced pressure and filtered through a column of neutral alumina (activity III, 7 cm length, 2.5 cm internal diameter) cooled to −50 °C. The orange filtrate was evaporated to dryness at 0 °C, and to the orange-red solid residue was added toluene (6 mL). The

(17) Bennett, M. A. In *Comprehensive Organometallic Chemistry II*; Abel, E. W., Stone, F. G. A., Wilkinson, G., Eds.; Pergamon: Oxford, 1995; Vol. 7, p 549.
(18) Bennett, M. A.; Neumann, H.; Thomas, M.; Wang, X.; Pertici, P.; Salvadori, P.; Vitulli, G. *Organometallics* **1991,** *10*, 3237.
(19) Pertici, P.; Ballantini, V.; Salvadori, P.; Bennett, M. A. *Organometallics* **1995**, *14*, 2565.
(20) Gordon, J. G. II; O'Connor, M. J.; Holm, R. H. *Inorg. Chim. Acta* **1971**, *5*, 381.
(21) Earley, J. E.; Base, R. N.; Berrie, B. H. *Inorg. Chem.* **1983**, *22*, 1836.
(22) Knowles, T. S.; Howells, M. E.; Howlin, B.; Smith, G. W.; Amodio, C. A. *Polyhedron* **1994**, *13*, 2197.
(23) Morris, G. A.; Freeman, R. *J. Magn. Reson.* **1978**, *29*, 433.
(24) *teXsan: Single Crystal Structure Analysis Software*, Versions 1.6c and 1.7; Molecular Structure Corp.: The Woodlands, TX, 1993, 1995.
(25) Cromer, D. T.; Waber, J. T. *International Tables for X-ray Crystallography*; Kynoch Press: Birmingham, England, 1974; Vol. IV.
(26) Creagh, D. C.; McAuley, W. J. *International Tables for Crystallography;* Kluwer Academic: Boston, MA, 1992; Vol. C, p 219.
(27) Creagh, D. C.; Hubbell, J. H. *International Tables for Crystallography*; Kluwer Academic: Boston, MA, 1992; Vol. C, p 200.
(28) Beurskens, P. T.; Admiraal, G.; Beurskens, G.; Bosman, W. P.; de Gelder, R.; Israel, R.; Smits, J. M. M. The DIRDIF-94 Program System. Technical Report of the Crystallography Laboratory; University of Nijmegen: Nijmegen, The Netherlands, 1994.

Table 1. Crystal and Refinement Data for $Ru(C_8H_8)_2$ (2) and $Ru(L)(C_8H_8)_2$ (L = CO (4), CN-*t*-Bu (5), PMe_3 (7))

	2	4	5	7
		(a) Crystal Data		
chemical formula	$C_{16}H_{16}Ru$	$C_{17}H_{16}ORu$	$C_{21}H_{25}NRu$	$C_{19}H_{25}PRu$
fw	309.37	337.38	392.51	385.45
cryst syst	orthorhombic	monoclinic	monoclinic	monoclinic
space group	*Pbca* (No. 61)	$P2_1/c$ (No. 14)	$P2_1/c$ (No. 14)	$P2_1/c$ (No.14)
crystal color, habit	red, lens	orange, needle	orange, prism	orange, block
a, Å	12.067(2)	11.172(4)	9.249(2)	11.570(2)
b, Å	12.359(2)	9.296(3)	16.796(2)	11.347(2)
c, Å	16.760(2)	13.407(4)	12.625(3)	13.199(1)
β, deg		91.17 (3)	103.77(2)	100.669(10)
V, Å^3	2499.6(6)	1392.1(7)	1905.0(8)	1702.8(4)
Z	8	4	4	4
ρ_{calc},g cm^{-3}	1.644	1.610	1.368	1.503
μ[Mo Kα], cm^{-1}	12.0	10.9	8.2	10.1
T, K	293(1)	293(1)	293(1)	293(1)
cryst dimens, mm	0.24 × 0.10 × 0.23	0.34 × 0.15 × 0.12	0.19 × 0.19 × 0.39	0.10 × 0.20 × 0.22
F(000)	1248	680	808	792
		(b) Data Collection and Processing		
diffractometer	Rigaku AFC6S	Rigaku AFC6S	Rigaku AFC6S	Rigaku AFC6S
X-radiation	Mo Kα	Mo Kα	Mo Kα	Mo Kα
λ, Å	0.710 69	0.710 69	0.710 69	0.710 69
scan mode	$\theta-2\theta$	$\theta-2\theta$	$\theta-2\theta$	$\theta-2\theta$
ω-scan width	1.20 + 0.34 tan θ	1.70 + 0.34 tan θ	1.30 + 0.34 tan θ	1.20 + 0.34 tan θ
scan rate, deg min^{-1} [a]	4	4	4	4
$2\theta_{max}$, deg	55.1	55.1	55.1	55.1
no. of unique data	2841	3426	4550	4135
no. of data refined	1442 [$I > 3\sigma(I)$]	1766 [$I > 3\sigma(I)$]	3401 [$I > 3\sigma(I)$]	3256 [$I > 3\sigma(I)$]
no. of variables	155	220	292	266
abs corr	analytical	analytical	analytical	analytical
min, max corr	0.78−0.90	0.85−0.89	0.85−0.89	0.80−0.85
		(c) Structure Analysis and Refinement[b]		
structure soln	Patterson and diff Fourier techniques (DIRDIF94, PATTY)[c]	Patterson and diff Fourier techniques (DIRDIF94, PATTY)[c]	Patterson and diff Fourier techniques (DIRDIF94, PATTY)[c]	Patterson and diff Fourier techniques (DIRDIF94, PATTY)[c]
refinement	full-matrix least-squares minimizing $\sum w(\|F_o\| - \|F_c\|)^2$	full-matrix least-squares minimizing $\sum w(\|F_o\| - \|F_c\|)^2$	full-matrix least-squares minimizing $\sum w(\|F_o\| - \|F_c\|)^2$	full-matrix least-squares minimizing $\sum w(\|F_o\| - \|F_c\|)^2$
weighting scheme *w*	$[\sigma^2(F) + (10^{-4})F^2]^{-1}$	$[\sigma^2(F) + (6 \times 10^{-6})F^2]^{-1}$	$[\sigma^2(F) + (10^{-6})F^2]^{-1}$	$[\sigma^2(F) + (10^{-4})F^2]^{-1}$
R	0.051	0.050	0.031	0.020
R_w	0.064	0.043	0.034	0.024
GOF	2.48	3.56	3.16	1.27

[a] Weak reflections were scanned up to four times and counts were accumulated. [b] Calculations were performed by use of teXsan,[24] with neutral atom scattering factors from ref 25, $\Delta f'$ and $\Delta f''$ values from ref 26, and mass attenuation coefficients from ref 27. [c] Reference 28.

solution was warmed to *ca.* 50 °C, treated with hexane (5 mL), and set aside at 0 °C. The large wine-red crystals that separated were washed with cold hexane (2 × 10 mL). The yield was *ca.* 70%. ^{1}H NMR (C_6D_6, 25 °C): δ 5.1 (br). $^{13}C\{^1H\}$ NMR (C_6D_6, 25 °C): δ 97 (br). EI-MS (70 eV): *m*/*z* 308.9 (M), 282.9 (M − C_2H_2), 203.9 (M − C_8H_8), 179.9. IR (KBr, cm^{-1}): 3010 (m), 2950 (m, C−H stretch), 1675 (m, uncoordinated C═C stretch), 1520 (w), 1465 (m), 1425 (m), 1380 (m), 1255 (m), 1140 (m), 975 (w), 915 (w), 860 (s), 840 (w), 820 (w), 795 (s), 780 (w), 705 (vs), 640 (w), 560 (w), 430 (w), 395 (w). Anal. Calcd for $C_{16}H_{16}Ru$: C, 62.12; H, 5.21. Found: C, 62.13; H, 5.35.

Bis(cyclooctatetraene)carbonylruthenium(0), Ru(CO)-((1−4-η)-C_8H_8)((1,2,5,6-η)-C_8H_8) (4). A magnetically stirred suspension of **2** (200 mg, 0.65 mmol) in hexane (40 mL) in a 100 mL two-necked flask was treated with CO (2 bar). The reaction was followed by monitoring the growth of the intense band at 2017 cm^{-1} in the IR spectrum and was complete after *ca.* 1 h. The solution was filtered through Celite, evaporated under reduced pressure to *ca.* 10 mL, and cooled to −30 °C overnight. The product was washed with cold hexane to give **4** as an orange-brown solid (165 mg, 75%). ^{1}H NMR (C_6D_6, 25 °C): δ 2.96 (d, 1H, J = 6 Hz), 3.89 (d, 1H, J = 6 Hz), 5.40 (s, 1H), 5.97(s, 1H, (1,2,5,6-η)-C_8H_8), 2.15 (br, 1H), 4.75(br, 1H), 5.6 (br, 2H, (1−4-η)-C_8H_8). $^{13}C\{^1H\}$ NMR (C_6D_6, 25 °C): δ 82.2, 87.5, 134.0, 135.0 ((1,2,5,6-η)-C_8H_8), 56 (br), 98 (br), 118 (br), 131 (br, (1−4-η)-C_8H_8), 214.7 (CO). EI-MS (70 eV): *m*/*z* 337 (M), 309 (M − CO), 283 (M − CO − C_8H_8), 206 (M − CO − C_2H_2 − C_8H_8). IR (hexane, cm^{-1}): 2017 (vs, CO); (KBr, cm^{-1}) 1990 (vs, CO), 1645 (s, uncoordinated C═C stretch of (1,2,5,6-η)-C_8H_8), 1557 (s, uncoordinated C═C stretch of (1−4-η)-C_8H_8). Anal. Calcd for $C_{17}H_{16}ORu$: C, 60.52; H, 4.78. Found: C, 60.78; H, 4.82.

The corresponding ^{13}CO derivative was made similarly from **2** (30 mg, 0.1 mmol) in hexane (10 mL). The IR spectrum of the reaction solution showed ν(CO) bands at 2021 (w), 1970 (s), 1952 (w), and 1924 (w) cm^{-1}. The $^{13}C\{^1H\}$ NMR spectrum in C_6D_6 of the yellow solid obtained after removing the solvent showed an intense singlet at δ 214.7 due to $Ru(^{13}CO)(C_8H_8)_2$, as well as weak peaks at δ 219.2, 203.4, 202.8, 200.6, and 198.4.

Bis(cyclooctatetraene)(*tert*-butyl isocyanide)ruthenium(0), Ru(CN-*t*-Bu)((1−4-η)-C_8H_8)((1,2,5,6-η)-C_8H_8) (5). To a suspension of 167 mg (0.54 mmol) of **2** in hexane (60 mL) was added from a syringe CN-*t*-Bu (0.094 mL, 0.84 mmol). The color changed to light brown within 10 min. After the mixture was stirred overnight at 0 °C, it was filtered through Celite. The bright yellow filtrate was reduced in volume to *ca.* 10 mL to give rust-brown crystals (76 mg), which were separated by filtration. A further 60 mg was obtained by cooling the filtrate in dry ice. The yield of **5**, mp 137−143 °C, was 64%. The sample for microanalysis was crystallized again from hexane. ^{1}H NMR (C_6D_6, 25 °C): δ 3.07 (d, J = 8.0 Hz), 3.84 (d, J = 8.0 Hz), 5.75 (s), 6.25 (s, (1,2,5,6-η)-C_8H_8), 2.2 (br), 4.9 (br), 5.6 (br), 6.0 (br, (1−4-η)-C_8H_8), 1.12 (*t*-Bu). $^{13}C\{^1H\}$ NMR (C_6D_6,

25 °C): δ 76.9, 83.6, 135.1, 135.4 ((1,2,5,6-η)-C_8H_8), 58 (br), 98 (br), 118 (br), 131 (br, (1−4-η)-C_8H_8), 30.7(*t*-Bu). EI-MS (70 eV): *m*/*z* 393 (M), 309 (M − CN-*t*-Bu), 289 (M − C_8H_8). IR (hexane, cm^{-1}): 2151(vs, C≡N stretch); (KBr, cm^{-1}) 2150 (vs), 1640 (s, uncoordinated C=C stretch of (1,2,5,6-η)-C_8H_8), 1570 (s, coordinated C=C stretch of (1−4-η)-C_8H_8). Anal. Calcd for $C_{21}H_{25}NRu$: C, 64.28; H, 6.37; N, 3.57. Found: C, 63.76; H, 5.98; N, 2.92.

Bis(cyclooctatetraene)(trimethyl phosphite)ruthenium(0), Ru{P(OMe)$_3$}((1−4-η)-C_8H_8)((1,2,5,6-η)-C_8H_8) (6). Addition of trimethyl phosphite (0.1 mL, 0.85 mmol) from a syringe to a suspension of **2** (247 mg, 0.80 mmol) in hexane (85 mL) caused a color change from orange to yellow within 5 min. The mixture was stirred for 2 h and filtered through Celite. The bright yellow filtrate was evaporated to *ca.* 20 mL and set aside at 0 °C to give orange, chunky crystals, which were washed with hexane (3 × 5 mL) at −78 °C and dried in vacuo. The yield of **6**, mp 117−120 °C, was 243 mg (70%). ^{1}H NMR (C_6D_6, 25 °C): δ 2.83 (d, J = 8.6 Hz), 3.87 (dd, J = 10.4, 8.6 Hz), 5.71 (s), 6.09 (s, (1,2,5,6-η)-C_8H_8), 2.30 (br, 1H), 4.85 (br, 1H), 5.50 (br, 1H), 5.84 (br, 1H, (1−4-η)-C_8H_8), 3.30 (d, 9H, J= 9 Hz, OMe). ^{13}C{^{1}H} NMR (C_6D_6, 25 °C): δ 52.0 (d, J_{PH} = 6.6 Hz), 76.2 (d, J_{PH} = 7.9 Hz), 84.8 (d, J_{PH} = 4.8 Hz), 134.8 (s, (1,2,5,6-η)-C_8H_8), 54.7 (br), 97.5 (br), 118.2 (br), 132.1 (br, (1−4-η)-C_8H_8), 134.7 (d, J_{PH} = 12.6 Hz, OMe). ^{31}P{^{1}H} NMR(C_6D_6): δ 162.3. EI-MS (70 eV): *m*/*z* 434 (M), 330 (M − C_8H_8). IR (KBr, cm^{-1}): 1640 (s, uncoordinated C=C stretch of (1,2,5,6-η)-C_8H_8), 1575 (uncoordinated C=C stretch of 1,4η-C_8H_8), 1055 (vs), 1045 (vs), 1015 (vs, C−O−C). Anal. Calcd for $C_{19}H_{25}O_3PRu$: C, 52.65; H, 5.77; P, 7.16. Found: C, 52.83; H, 6.00; P, 6.91.

The complexes Ru(L)((1−4-η)-C_8H_8)((1,2,5,6-η)-C_8H_8) (L = PMe_3(**7**), PEt_3 (**8**)) were prepared similarly to **6** as red-brown, crystalline solids in *ca.* 70% yield, mp 146−149 °C and 128−132 °C, respectively.

7: ^{1}H NMR (C_6D_6) δ 1.34 (d, J_{PH} = 8.6 Hz, Me), 2.67 (d, J_{PH} = 8.6 Hz), 3.24 (dd, separation = 9.1 Hz), 5.73 (s), 5.92 (s, (1,2,5,6-η)-C_8H_8), 2.1 (br), 4.7 (br), 5.4 (br), 5.8 (br, (1−4-η)-C_8H_8). ^{13}C{^{1}H} NMR (C_6D_6): δ 21.2 (d, J_{PC} = 26 Hz, Me), 74.1 (d, J_{PC} = 5.8 Hz), 83.9 (d, J_{PC} = 3.0 Hz), 135.3 (s), 135.4 (s, (1,2,5,6-η)-C_8H_8), 55.1 (br), 98.0 (br), 118.0 (br), 134.2 (br, (1−4-η)-C_8H_8). ^{31}P{^{1}H} NMR (C_6D_6): δ 4.9. EI-MS (70 eV): *m*/*z* 386 (M), 309 (M − PMe_3), 282 (M − C_8H_8). IR (KBr, cm^{-1}): 1640 (s, uncoordinated C=C stretch of (1,2,5,6-η)-C_8H_8), 1570 (s, uncoordinated C=C stretch of (1−4-η)-C_8H_8), 1480 (s), 1450 (s), 1410 (s), 1350 (s), 1300 (m). Anal. Calcd for $C_{19}H_{25}PRu$: C, 59.22; H, 6.49; P, 8.05. Found: C, 59.01; H, 6.67; P, 6.98.

8: ^{1}H NMR(C_6D_6) δ 0.83 (quint, separation = 7.4 Hz, Me), 1.90 (quint, separation = 7.6 Hz, CH_2), 2.69 (d, J_{PH} = 8.7 Hz), 3.56 (t, separation = 9.0 Hz), 5.75 (s), 5.90 (s, (1,2,5,6-η)-C_8H_8), 2.3 (br), 4.8 (br), 5.4 (br), *ca.* 5.9 (br, (1−4-η)-C_8H_8). ^{13}C{^{1}H} NMR (C_6D_6): δ 8.15 (s, Me), 19.4 (d, J_{PC} = 22 Hz, CH_2), 72.3 (d, J_{PC} = 6.1 Hz), 84.4 (s), 135.1 (s), 135.2 (s, (1,2,5,6-η)-C_8H_8), 54.5 (br), 97.5 (br), 118.0 (br), 133.7 (br, (1−4-η)-C_8H_8). ^{31}P{^{1}H} NMR (C_6D_6): δ 25.1. EI-MS (70 eV): *m*/*z* 428 (M), 324 (M − C_8H_8), 309 (M − PEt_3). IR (KBr, cm^{-1}): 1640 (m, uncoordinated C=C stretch of (1,2,5,6-η)-C_8H_8), 1570 (m, uncoordinated C=C stretch of (1−4-η)-C_8H_8). Anal. Calcd for $C_{22}H_{31}Ru$: C, 61.82; H, 7.26; P, 7.26. Found: C, 61.54; H, 7.49; P, 7.19.

Results

Routes to Ru(C_8H_8)$_2$ (**2**) based on the reactions of COT/Et_3Al or K_2[COT] with $RuCl_3$ did not look promising because of the notorious inertness of anhydrous $RuCl_3$ and the presence of water in the so-called hydrated $RuCl_3$. We, therefore, started from Ru(acac)$_3$, which can be made easily in high yield from hydrated $RuCl_3$. Attempts to isolate **2** from the direct reaction of Ru(acac)$_3$ with an excess of K_2[COT] were unsuccessful. However, reduction of Ru(acac)$_3$ with zinc amalgam in refluxing THF containing a small amount of water[29] and a large excess of COT gives almost quantitatively a yellow-brown solid, Ru(acac)$_2$(C_8H_8) (**3**), which contains a parent ion in its EI mass spectrum. The ^{1}H NMR spectrum shows a pair of doublets of doublets due to uncoordinated olefinic protons in the region δ 6.1−6.3 and a similar pair of resonances assignable to coordinated olefinic protons in the region δ 4.0−4.5. There are also a pair of singlets between δ 1.5 and 2.0 due to inequivalent methyl groups of acac and a singlet at δ 5.19 due to the acac γ-protons. These data indicate that Ru(II) is coordinated octahedrally by tub-shaped (1,2,5,6-η)-COT and a pair of mutually *cis*-acac ligands, similar to the corresponding 1,5-COD and NBD complexes.[30,31]

Treatment of **3** with K_2[COT] in ether between −78 and −30 °C over a period of *ca.* 12 h and subsequent chromatography on alumina at −50 °C gives Ru(C_8H_8)$_2$ (**2**) as a bright red, crystalline solid in yields of 60−70% after recrystallization from toluene or hexane. To obtain these yields, it is important not to allow the temperature to rise to 0 °C during the reaction and to use ether rather than THF as the reaction medium, otherwise decomposition occurs. Once isolated, however, **2** is stable as a solid in an inert atmosphere for several days and even, for a short time, in air. Solutions in hexane are stable for days in the absence of air, but in benzene, toluene, ether, or THF, decomposition occurs after several hours at room temperature, giving COT as the only organic product. The EI mass spectrum shows a parent ion accompanied by peaks due to loss of C_2H_2 and C_8H_8.

At room temperature in C_6D_6 or CD_2Cl_2, the NMR spectra (^{1}H, ^{13}C) consist of one broad peak. On cooling a toluene-d_8 solution to −50 °C, the ^{1}H NMR spectrum shows four resonances at δ 5.47, 4.90, 4.54, and 4.53 in a ratio of 10:2:2:2, which are similar to those observed for Fe((1−6-η)-C_8H_8)((1−4-η)-C_8H_8) (**1**);[12] they correspond to the four 2H signals expected for a "frozen" (1−6-η)-C_8H_8 ring and the 8H singlet arising from a (1−4-η)-C_8H_8 ring that is still fluxional at −50 °C. Better peak separation and spectra are obtained in CD_2Cl_2; at about −70 °C, four well-resolved multiplets due to the (1−6-η)-C_8H_8 protons are observed at δ 6.24, 5.22, 5.15, and 5.05 and a sharp singlet due to the rapidly exchanging (1−4-η)-C_8H_8 protons at δ 5.40 (Figure 1). The resonance at δ 6.24 is the A part of an [AMNX]$_2$ pattern, which, owing to the absence of significant AN coupling, appears as a typical A part of a [AX]$_2$ multiplet. On the basis of its pattern and chemical shift, it must be due to the uncoordinated pair of CH protons, H^4 (see Figure 2 for numbering of protons and carbon atoms). This assignment has been confirmed by ^{13}C−{^{1}H} correlation (see below). The signal at δ 5.21(H^3) mirrors the pattern for H^4 and is split further into a leaning

(29) This procedure can also be used to generate labile species Ru(acac)$_2$(alkene)$_2$ (alkene = cyclooctene, C_2H_4), which are useful precursors to a range of Ru(acac)$_2L_2$ complexes, see: Bennett, M. A.; Chung, G.; Neumann, H. Unpublished work. A similar procedure employing zinc dust in ethanol has been used to prepare Ru(acac)$_2$(η^4-diene) complexes, see: Ernst, R. D.; Meléndez, E.; Stahl, L.; Ziegler, M. L. *Organometallics* **1991**, *10*, 3635. Meléndez, E.; Ilarraza, R.; Yap, G. P. A.; Rheingold, A. L. *J. Organomet. Chem.* **1996**, *522*, 1.

(30) Powell, P. *J. Organomet. Chem.* **1974**, *65*, 89.

(31) It should be noted that COT is reported to react directly with ethanolic $RuCl_3$ only in the presence of air to give a 1,3,5-cyclooctatriene complex [$RuCl_2$(η^6-1,3,5-C_8H_{10})]$_2$, not a COT complex, see: Toerien, J. G. *J. Organomet. Chem.* **1991**, *405*, C43.

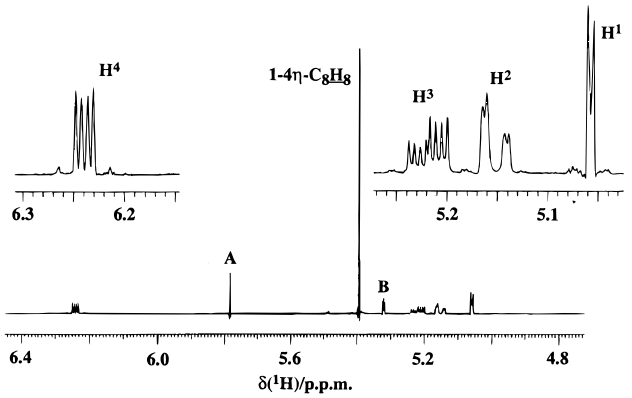

Figure 1. ^{1}H NMR spectrum at 400.13 MHz of Ru((1−6-η)-C_8H_8)((1−4-η)-C_8H_8) (**2**) in CD_2Cl_2 at −70 °C. Expansions of the multiplets due to the (1−6-η)-C_8H_8 protons are inset. Peaks marked A and B are due to free COT and $CHDCl_2$, respectively.

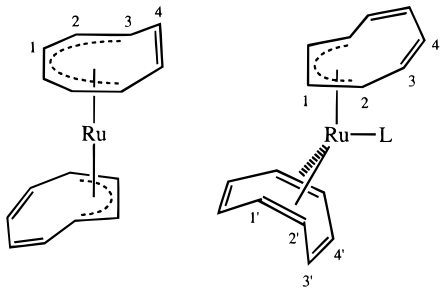

2 L = CO (**4**), *t*-BuNC (**5**), $P(OMe)_3$ (**6**), PMe_3 (**7**), PEt_3 (**8**)

Figure 2. Structures of Ru((1−6-η)-C_8H_8)((1−4-η)-C_8H_8) (**2**) and Ru(L)((1−4-η)-C_8H_8)((1,2,5,6-η)-C_8H_8) (L = CO (**4**), CN-*t*-Bu (**5**), $P(OMe)_3$ (**6**), PMe_3 (**7**), PEt_3 (**8**)) showing numbering of protons and carbon nuclei.

doublet because of coupling with the signal at δ 5.15 (H^2), which shows a small coupling to the resonance at δ 5.06 (H^1). This interpretation was confirmed by decoupling experiments. Correspondingly, the $^{13}C\{^1H\}$ NMR spectra at −60 °C show four singlets due to the "frozen" (1−6-η)-C_8H_8 carbon atoms at δ 135.1, 98.7, 91.5, and 78.2 (toluene-d_8) (134.7, 98.3, 91.3, and 78.3 (CD_2Cl_2)) and a singlet at δ 95.6 (toluene-d_8) (94.5 (CD_2Cl_2)) due to the (1−4-η)-C_8H_8 carbon atoms. The protons were tied to the carbon atoms by a 2-D CH correlation experiment on the CD_2Cl_2 solution. The signal at δ 134.7 can be assigned unambiguously to the uncoordinated C^4 on the basis of its chemical shift, which is very close to that of free COT at δ 131.7. This resonance is connected to that at δ 6.24, due to H^4. The remaining assignments of the (1−6-η)-C_8H_8 ring are δ 91.3 (C^3), 78.3 (C^2), and 98.3 (C^1).

The structural similarity of **1** and **2** is confirmed by the X-ray structural analysis of **2** (see below) and is also evident from a comparison of their IR spectra. Absorptions at 1675 and 1520 cm^{-1} in the spectrum of **2** can be assigned to the ν(C═C) vibrations of the uncoordinated double bonds of (1−6-η)-C_8H_8 and (1−4-η)-C_8H_8, respectively; the ν(C═C) bands due to the coordinated double bonds appear at 1465 and 1440 cm^{-1}. The corresponding absorptions in **1** are at 1662, 1527, 1468, and 1437 cm^{-1}.[10]

Complex **2** reacts rapidly with CO to give an orange, air-stable monocarbonyl complex Ru(CO)(C_8H_8)$_2$ (**4**) as the main product in 70% isolated yield. This shows one strong ν(CO) band in its IR spectrum at 2017 cm^{-1} (hexane) (1972 cm^{-1} in the ^{13}CO analogue). The EI mass spectrum shows a parent ion peak accompanied by fragments due to $M^+ - CO$ and $M^+ - CO - C_8H_8$. The IR spectrum of the reaction mixture formed from **2** and CO shows numerous additional weaker ν(CO) bands, including two at 2070 and 1996 cm^{-1}, which can be assigned to $Ru(CO)_3$((1−4-η)-C_8H_8);[32,33] the reported band at 2010 cm^{-1} for this compound is not observed, probably because it is masked by the intense absorption due to **4**. The proportion of these minor side-products does not increase if the reaction mixture is set aside under CO for 24 h. Thus the behavior of **2** with CO differs from that of **1**, which is reported to react with CO to give $Fe(CO)_3$((1−4-η)-C_8H_8) directly.[6]

The ^{1}H NMR spectrum of **4** at room temperature shows a pair of 1H singlets (δ 5.97, 5.40 (C_6D_6); 6.15, 5.60 (CD_2Cl_2)) and a pair of 1H doublets (J = 6 Hz) (δ 3.89, 2.96 (C_6D_6); 4.25, 3.49 (CD_2Cl_2)), whose appearance suggests the presence of a (1,2,5,6-η)-C_8H_8 ring, together with three broad resonances centered at δ 5.6 (2H), 4.75 (1H), and 2.15 (1H, C_6D_6), assignable to a fluxional (1−4-η)-C_8H_8 ring (see Figure 2, which shows the numbering of protons and carbon atoms). This pattern is mirrored in the $^{13}C\{^1H\}$ NMR spectrum, which shows sharp singlets at δ 135.0 and 134.0 (uncoordinated) and δ 87.5 and 82.2 (coordinated) arising from (1,2,5,6-η)-C_8H_8 and broad resonances at δ 131, 128, and 98 due to (1−4-η)-C_8H_8. There is also a ^{13}CO resonance at δ 214.5 (C_6D_6). The conclusions are confirmed by the X-ray structural determination (see below) and by the IR spectrum, which contains bands at 1645 and 1452 cm^{-1} assignable to ν(C═C) of the uncoordinated and coordinated fragments, respectively, of (1,2,5,6-η)-C_8H_8,[34] and a band at 1557 cm^{-1} assignable to the ν(C═C) mode of the uncoordinated part of (1−4-η)-C_8H_8 (*cf.* 1562 cm^{-1} in $Fe(CO)_3$((1−4-η)-C_8H_8)).[35]

The ^{1}H and ^{13}C NMR signals due to (1−4-η)-C_8H_8 coalesce when a toluene-d_8 solution of **4** is heated to *ca.* 60 °C and sharpen to four separate resonances when solutions in toluene-d_8 or CD_2Cl_2 are cooled to *ca.* −40 °C, whereas the (1,2,5,6-η)-C_8H_8 signals remain sharp over the entire temperature range. Decoupling experiments in CD_2Cl_2 confirmed the connectivity δ 6.15−4.23−3.49−5.60 for the protons of the (1,2,5,6-η)-ring and δ 5.24−2.42−5.83−5.29 for those of the (1−4-η)-ring. The assignment of these resonances has been assisted by NOE measurements.[36] Preirradiation of the signal at δ 3.49 causes substantial enhancements in the signals at δ 5.22 and 2.42 due to protons in the (1−4-η)-C_8H_8 ring, in addition to the expected enhancements in the (1,2,5,6-η)-ring at δ 5.60 and 4.23. Also, relayed negative NOEs are observed in the signals at δ 6.15, 5.83, and 5.29. Preirradiation of the signal at δ 4.23 causes little transfer to the ^{1}H resonances of the (1−4-η)-ring and only a small enhancement at δ 2.42. Examination of the X-ray structure of **4** (see below)

(32) Bruce, M. I.; Cooke, M.; Green, M. *J. Organomet. Chem.* **1968**, *13*, 227.
(33) Cotton, F. A.; Davison, A.; Marks, T. J.; Musco, A. *J. Am. Chem. Soc.* **1969**, *91*, 6598.
(34) Bennett, M. A.; Saxby, J. D. *Inorg. Chem.* **1968**, *7*, 321.
(35) Bailey, R. T.; Lippincott, E. R.; Steele, D. *J. Am. Chem. Soc.* **1965**, *87*, 5346.
(36) Sanders, J. K. M.; Mersh, J. D. *Prog. NMR Spectrosc.* **1986**, *69*, 92.

shows that, on average, the $H^{1'}$ proton of the (1,2,5,6-η)-C_8H_8 ring is separated from H^1 and H^2 of the (1−4-η)-C_8H_8 ring by 2.50 Å and 2.49 Å, respectively; proton $H^{2'}$ is at an average of 2.92 Å from H^2 and over 4 Å from H^1 and H^3 of the (1−4-η)-C_8H_8 ring. This is consistent with the NOE experiment if the peaks at δ 3.49 and δ 4.23 are due to $H^{1'}$and $H^{2'}$, respectively. The NOE and decoupling results complete the assignment of the (1,2,5,6-η)-C_8H_8 protons with $H^{3'}$ at δ 6.15 and $H^{4'}$ at δ 5.60.

At 233 K, the ^{13}C NMR spectrum of **4** is sharp and can be assigned on the basis of a 2-D $^{13}C\{^1H\}$ NMR spectrum and literature comparisons as follows: δ 134.6, 133.7 ($C^{3'}$, $C^{4'}$ of (1,2,5,6-η)-C_8H_8), 130.9 (C^3 of (1−4-η)-C_8H_8), 116.7 (C^4 of (1−4-η)-C_8H_8), 97.7 (C^1 of (1−4-η)-C_8H_8), 87.3, 82.2 ($C^{1'}$, $C^{2'}$of (1,2,5,6-η)-C_8H_8), and 55.9 (C^2 of (1−4-η)-C_8H_8).

Other π-acceptor ligands also react with **2** to give orange-yellow, air-stable complexes Ru(L)((1−4-η)-C_8H_8)-((1,2,5,6-η)-C_8H_8) (L = CN-*t*-Bu (**5**), $P(OMe)_3$ (**6**), PMe_3 (**7**), and PEt_3 (**8**)). The ^1H and ^{13}C NMR spectra of the C_8H_8 ligands in **5**−**8** at room temperature resemble those in **3**, and the structures of **4**, **5**, and **7** determined by X-ray crystallography (see below) are similar. The mass spectra of **5**−**8**, like those of **3**, exhibit parent ion peaks together with peaks due to $[M - L]^+$ and $[M - L - C_8H_8]^+$. The ^1H NMR spectrum of **2** in CD_3CN at room temperature is similar to that in C_6D_6 or CD_2Cl_2; hence, there is no evidence for the formation of a solvate species Ru((1−4-η)-C_8H_8)((1,2,5,6-η)-C_8H_8)-($NCCD_3$). There is also no reaction between **2** and ethylene (1 bar).

X-ray Structural Analysis. The molecular structure of Ru((1−6-η)-C_8H_8)((1−4-η)-C_8H_8) (**2**) is shown in Figure 3; important bond lengths and angles are summarized in Table 2. Caution is necessary in the discussion of these parameters, especially the C−C distances, because the correction for the stacking fault (see Experimental Section) may not have removed all of the resulting systematic error.

The crystals of **1** and **2** are not isomorphous. Whereas all molecules in the orthorhombic unit cell of **2** are well-defined, the monoclinic unit cell of **1** contains two nonequivalent molecules, one of which is strongly disordered.[10,11] The molecular structures of **1** and **2** differ mainly in the relative orientation of the rings. In **2**, the angle between the plane including the metal atom/the midpoint of C3−C4 (the central coordinated double bond of (1−6-η)-C_8H_8)/the midpoint of C7−C8 (the uncoordinated double bond of (1−6-η)-C_8H_8) and the plane defined by the metal atom/the midpoint of C10−C11 (the center of the coordinated part of (1−4-η)-C_8H_8)/the midpoint of C14−C15 (the center of the uncoordinated part of (1−4-η)-C_8H_8) is 157°, whereas the corresponding angle in **1** is 68°.[10] The metal-bound carbon atoms of the η^6-ring of **2** are approximately coplanar, although the separations between the ruthenium atom and the central carbon atoms C(3), C(4) (2.27(1), 2.25(1) Å) appear to be significantly greater than those to C(1), C(2), C(5), and C(6) (2.14(1), 2.15(1), 2.17(1), 2.21(1) Å, respectively). In contrast, in $Mo(CO)_3$-((1−6-η)-C_8H_8)[37] and $Cr(CO)_3$((1−6-η)-1,3,5,7-$C_8H_4Me_4$),[38]

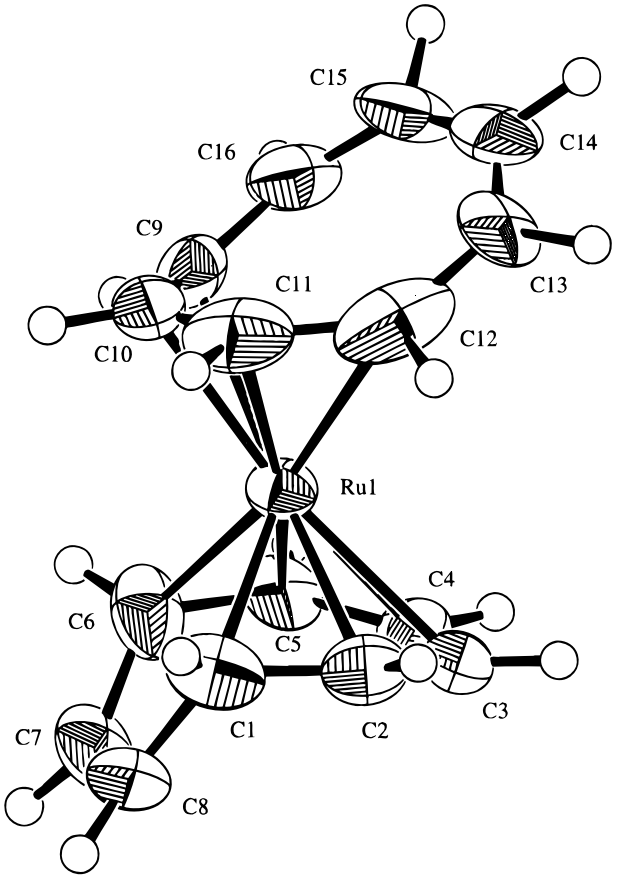

Figure 3. Molecular structure of Ru((1−6-η)-C_8H_8)((1−4-η)-C_8H_8) (**2**). Thermal ellipsoids are at the 50% probability level. Hydrogen atoms are drawn as small circles of arbitrary radius.

the distances from the metal atom to both terminal carbon atoms appear to be greater than those to the inner carbon atoms. The Ru−C bond lengths to the (1−6-η)-ring of **2** are generally similar to those observed to (1−6-η)-1,3,5-cyclooctatriene in Ru((1−6-η)-1,3,5-C_8H_{10})-((1,2,5,6-η)-C_8H_{12}).[39] In the (1−4-η)-ring, the Ru-C distances to the outer carbon atoms of the bound diene fragment (Ru−C(9) 2.34(1) Å, Ru−C(12) 2.42(1) Å) are significantly greater than those to the inner carbon atoms (Ru−C(10) 2.11(1) Å, Ru−C(11) 2.10(1) Å). A similar but less pronounced trend is observed in Ru-$(CO)_3$((1−4-η)-C_8H_8)[40] and Ru(η^6-C_6Me_6)((1−4-η)-C_8H_8).[41] Correspondingly, the C−C distances in the (1−4-η)-unit of **2** appear to show a long−short−long trend (1.48(2), 1.37(2), 1.44(2) Å), which is far less evident in $Ru(CO)_3$-((1−4-η)-C_8H_8) (1.443(8), 1.394(12), 1.443(8) Å)[40] and in Ru(η^6-C_6Me_6)((1−4-η)-C_8H_8) (1.413(16), 1.400(16), 1.423(15) Å).[41] The (1−6-η)-ring is hinged at C(1) and C(6), the dihedral angle between the mean planes C(1)−C(2)−C(3)−C(4)−C(5)−C(6) and C(6)−C(7)−C(8)−C(1) being 117° (*cf.* 130° in $Mo(CO)_3$((1−6-η)-C_8H_8)[37] and 119° in $Cr(CO)_3$((1−6-η)-1,3,5,7-$C_8H_4Me_4$)[38]). The (1−4-η)-ring is hinged at C(9) and C(12), the dihedral angle between the mean planes C(9)−C(10)−C(11)−C(12) and C(12)−C(13)−C(14)−C(15)−C(16)−C(19) being 147° (*cf.* 147° in **1**,[10] 136° in $Ru(CO)_3$((1−4-η)-C_8H_8),[40] 138° in Fe-

(37) McKechnie, J. S.; Paul, I. C. *J. Am. Chem. Soc.* **1966**, *88*, 5927.
(38) Bennett, M. J.; Cotton, F. A.; Takats, J. *J. Am. Chem. Soc.* **1968**, *90*, 903.
(39) Frosin, K-M.; Dahlenburg, L. *Inorg. Chim. Acta* **1990**, *167*, 83.
(40) Cotton, F. A.; Eiss, R. *J. Am. Chem. Soc.* **1969**, *91*, 6593.
(41) Bennett, M. A.; Matheson, T. W.; Robertson, G. B.; Smith, A. K.; Tucker, P. A. *Inorg. Chem.* **1980**, *19*, 1014.

Table 2. Selected Interatomic Distances (Å) and Angles (deg) for Ru((1−6-η)-C_8H_8)((1−4-η)-C_8H_8) (2)

Ru(1)−C(1)	2.14(1)	Ru(1)−C(2)	2.15(1)
Ru(1)−C(3)	2.27(1)	Ru(1)−C(4)	2.25(1)
Ru(1)−C(5)	2.17(1)	Ru(1)−C(6)	2.21(1)
Ru(1)−C(9)	2.34(1)	Ru(1)−C(10)	2.11(1)
Ru(1)−C(11)	2.10(1)	Ru(1)−C(12)	2.42(1)
C(1)−C(2)	1.37(2)	C(1)−C(8)	1.43(2)
C(2)−C(3)	1.42(2)	C(3)−C(4)	1.46(2)
C(4)−C(5)	1.39(2)	C(5)−C(6)	1.35(2)
C(6)−C(7)	1.47(2)	C(7)−C(8)	1.39(2)
C(9)−C(10)	1.48(2)	C(9)−C(16)	1.38(2)
C(10)−C(11)	1.37(2)	C(11)−C(12)	1.44(2)
C(12)−C(13)	1.37(2)	C(13)−C(14)	1.30(2)
C(14)−C(15)	1.37(2)	C(15)−C(16)	1.28(2)
C(1)−Ru(1)−C(2)	37.3(5)	C(1)−Ru(1)−C(3)	69.9(6)
C(1)−Ru(1)−C(4)	92.5(5)	C(1)−Ru(1)−C(5)	99.0(5)
C(1)−Ru(1)−C(6)	78.7(5)	C(1)−Ru(1)−C(9)	141.4(5)
C(1)−Ru(1)−C(10)	109.0(6)	C(1)−Ru(1)−C(11)	93.7(5)
C(1)−Ru(1)−C(12)	104.9(5)	C(2)−Ru(1)−C(3)	37.5(4)
C(2)−Ru(1)−C(4)	71.6(5)	C(2)−Ru(1)−C(5)	97.7(5)
C(2)−Ru(1)−C(6)	98.5(6)	C(2)−Ru(1)−C(9)	171.3(5)
C(2)−Ru(1)−C(10)	134.1(6)	C(2)−Ru(1)−C(11)	101.5(6)
C(2)−Ru(1)−C(12)	89.7(5)	C(3)−Ru(1)−C(4)	37.7(4)
C(3)−Ru(1)−C(5)	72.0(5)	C(3)−Ru(1)−C(6)	92.3(5)
C(3)−Ru(1)−C(9)	147.7(5)	C(3)−Ru(1)−C(10)	164.6(5)
C(3)−Ru(1)−C(11)	127.0(6)	C(3)−Ru(1)−C(12)	97.9(5)
C(4)−Ru(1)−C(5)	36.5(4)	C(4)−Ru(1)−C(6)	66.9(5)
C(4)−Ru(1)−C(9)	116.0(5)	C(4)−Ru(1)−C(10)	154.2(6)
C(4)−Ru(1)−C(11)	158.2(6)	C(4)−Ru(1)−C(12)	121.8(5)
C(5)−Ru(1)−C(6)	35.9(4)	C(5)−Ru(1)−C(9)	91.0(5)
C(5)−Ru(1)−C(10)	122.8(6)	C(5)−Ru(1)−C(11)	160.3(6)
C(5)−Ru(1)−C(12)	149.0(6)	C(6)−Ru(1)−C(9)	88.7(5)
C(6)−Ru(1)−C(10)	102.7(5)	C(6)−Ru(1)−C(11)	134.9(6)
C(6)−Ru(1)−C(12)	169.8(5)	C(9)−Ru(1)−C(10)	38.4(5)
C(9)−Ru(1)−C(11)	69.8(5)	C(9)−Ru(1)−C(12)	82.6(4)
C(10)−Ru(1)−C(11)	37.8(5)	C(10)−Ru(1)−C(12)	67.2(5)
C(11)−Ru(1)−C(12)	36.4(5)	Ru(1)−C(1)−C(2)	71.5(7)
Ru(1)−C(1)−C(8)	115(1)	C(2)−C(1)−C(8)	123(1)
Ru(1)−C(2)−C(1)	71.2(7)	Ru(1)−C(2)−C(3)	75.9(7)
C(1)−C(2)−C(3)	129(1)	Ru(1)−C(3)−C(2)	66.7(7)
Ru(1)−C(3)−C(4)	70.5(7)	C(2)−C(3)−C(4)	127(1)
Ru(1)−C(4)−C(3)	71.7(7)	Ru(1)−C(4)−C(5)	68.4(6)
C(3)−C(4)−C(5)	133(1)	Ru(1)−C(5)−C(4)	75.1(7)
Ru(1)−C(5)−C(6)	73.7(7)	C(4)−C(5)−C(6)	128(2)
Ru(1)−C(6)−C(5)	70.5(7)	Ru(1)−C(6)−C(7)	109.8(9)
C(5)−C(6)−C(7)	125(1)	C(6)−C(7)−C(8)	120(1)
C(1)−C(8)−C(7)	116(1)	Ru(1)−C(9)−C(10)	62.3(6)
Ru(1)−C(9)−C(16)	116.3(8)	C(10)−C(9)−C(16)	133(1)
Ru(1)−C(10)−C(9)	79.3(7)	Ru(1)−C(10)−C(11)	71.1(7)
C(9)−C(10)−C(11)	127(1)	Ru(1)−C(11)−C(10)	71.1(7)
Ru(1)−C(11)−C(12)	83.7(8)	C(10)−C(11)−C(12)	127(1)
Ru(1)−C(12)−C(11)	60.0(6)	Ru(1)−C(12)−C(13)	116.9(9)
C(11)−C(12)−C(13)	138(1)	C(12)−C(13)−C(14)	132(1)
C(13)−C(14)−C(15)	134(1)	C(14)−C(15)−C(16)	136(1)
C(9)−C(16)−C(15)	133(1)		

($CO)_3$((1−4-η)-C_8H_8),[42] 135° in Ru(η^6-C_6Me_6)((1−4-η)-C_8H_8),[41] and 137° in Fe(CO)((1−4-η)-C_8H_8)((1−4-η)-C_4H_6).[43])

In agreement with the conclusions based on the spectroscopic data, the complexes Ru(L)(C_8H_8)$_2$ (L = CO (**4**), CN-*t*-Bu (**5**), and PMe_3 (**7**)) each contain a (1,2,5,6-η)- and a (1−4-η)-C_8H_8 ring. Two views of the molecular structure of **7**, which is the most precisely determined structure, are shown in Figure 4. Important bond lengths for all three structures are summarized in Table 3. The coordination geometry for all three compounds can be described as approximately square pyramidal with L in the axial site; it is similar to that found in Fe(CO)((1−4-η)-C_8H_8)((1−4-η)-C_4H_6),[43] Ru{P($OMe)_3$}-((1−4-η)-1,3,5-C_8H_{10})(η^4-1,5-C_8H_{12}),[44] and Ru{P($OMe)_3$}-(*E*,*E*-$MeO_2CCH{=}CHCH{=}CHCO_2Me)_2$.[45] The planes of the bound carbon atoms of the two C_8H_8 rings are inclined to each other by 17° (**4**), 16° (**5**), and 27° (**7**). In

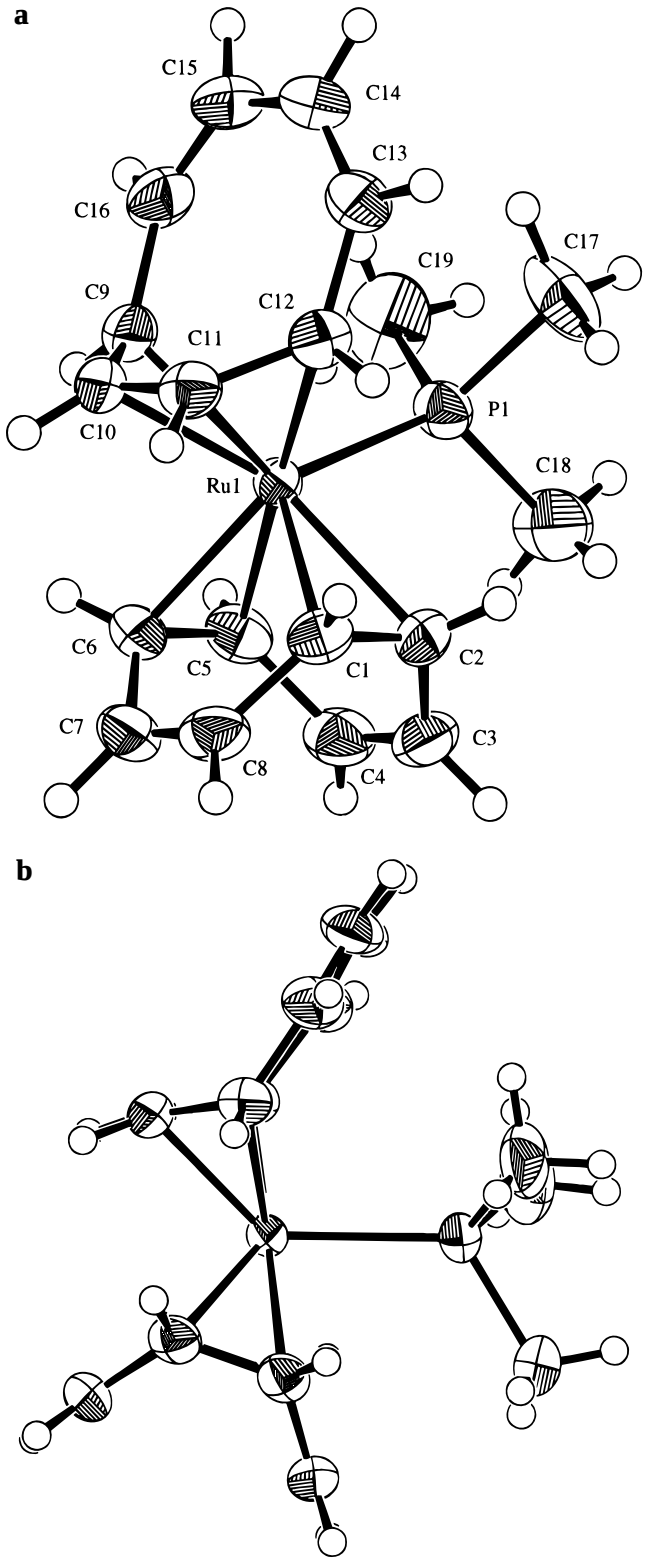

Figure 4. Two views of the molecular structure of Ru(PMe_3)((1−4-η)-C_8H_8)((1,2,5,6-η)-C_8H_8) (**7**). Thermal ellipsoids are at the 50% probability level. Hydrogen atoms are drawn as small circles of arbitrary radius.

(42) Dickens, B.; Lipscomb, W. N. *J. Chem. Phys.* **1962**, *37*, 2084.
(43) Bassi, I. W.; Scordamaglia, R. *J. Organomet. Chem.* **1972**, *37*, 353.
(44) Pertici, P.; Vitulli, G.; Porzio, W.; Zocchi, M.; Barili, P.; Deganello, G. *J. Chem. Soc., Dalton Trans.* **1983**, 1553.
(45) McKinney, R. J.; Colton, M. C. *Organometallics* **1986**, *5*, 1080.

Table 3. Selected Interatomic Distances (Å) in Ru(L)((1−4-η)-C_8H_8)((1,2,5,6-η)-C_8H_8) (L=CO(4),[a] CN-*t*-Bu(5),[b] PMe_3 (7)[c])

	4	5	7		4	5	7
Ru−C(1)	2.234(10)	2.189(4)	2.197(2)	Ru−C(2)	2.266(10)	2.211(4)	2.241(2)
Ru−C(5)	2.266(10)	2.228(4)	2.237(2)	Ru−C(6)	2.245(9)	2.198(4)	2.184(2)
Ru−C(9)	2.210(12)	2.225(4)	2.231(2)	Ru−C(10)	2.184(11)	2.173(4)	2.172(2)
Ru−C(11)	2.189(10)	2.173(4)	2.164(2)	Ru−C(12)	2.213(8)	2.223(4)	2.241(2)
C(1)−C(2)	1.398(14)	1.395(7)	1.407(3)	C(1)−C(8)	1.521(14)	1.497(7)	1.479(3)
C(2)−C(3)	1.505(14)	1.485(7)	1.490(3)	C(3)−C(4)	1.267(14)	1.301(7)	1.311(4)
C(4)−C(5)	1.453(14)	1.479(6)	1.480(4)	C(5)−C(6)	1.382(15)	1.402(6)	1.410(3)
C(6)−C(7)	1.469(16)	1.486(7)	1.487(3)	C(7)−C(8)	1.238(15)	1.287(7)	1.310(4)
C(9)−C(10)	1.421(16)	1.439(6)	1.434(3)	C(9)−C(16)	1.502(17)	1.463(6)	1.461(3)
C(10)−C(11)	1.389(15)	1.403(6)	1.395(3)	C(11)−C(12)	1.443(13)	1.442(6)	1.431(3)
C(12)−C(13)	1.480(15)	1.482(7)	1.472(3)	C(13)−C(14)	1.302(14)	1.333(7)	1.340(4)
C(14)−C(15)	1.389(14)	1.433(7)	1.421(4)	C(15)−C(16)	1.347(16)	1.346(7)	1.333(4)

[a] Ru−C(17) 1.852(10); C(17)−O(1) 1.171(9). [b] Ru−C(17) 1.984(4); C(17)−N(1) 1.150(5). [c] Ru−P(1) 2.3665(6); P(1)−C(17) 1.814(3); P(1)−C(18) 1.825(3); P(1)−C(19) 1.820(3).

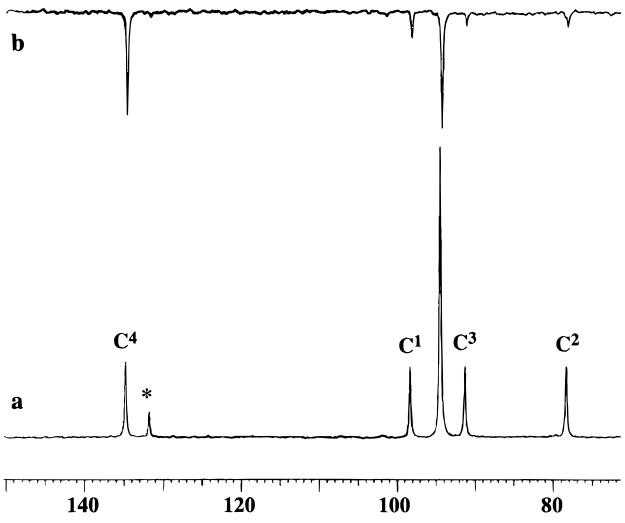

Figure 5. ^{13}C NMR spectrum at 100.62 MHz of Ru((1−6-η)-C_8H_8)((1−4-η)-C_8H_8) (**2**) in CD_2Cl_2 at −38 °C, using the pulse sequence given in the Experimental Section. The selective DANTE pulse was placed at δ 134.7. (a) Spectrum obtained with $\tau = 10$ s. (b) Spectrum obtained by subtracting spectrum a from the spectrum obtained with $\tau = 0.08$ s. The peak marked with an asterisk is due to free COT.

the tub-shaped (1,2,5,6-η)-rings, the separations between the metal atom and the coordinated olefinic carbon atoms fall into distinct pairs, Ru−C(1), Ru−C(6) 2.18−2.20 Å and Ru−C(2), Ru−C(5) 2.22−2.24 Å. As expected, the coordinated C=C distances are greater in all cases by 0.05−0.10 Å than the uncoordinated ones, as found also in $PdCl_2$ ((1,2,5,6-η)-C_8H_8).[46] The geometry of the (1−4-η)-C_8H_8 rings is similar to that in **2** and in the other (1−4-η)-C_8H_8 complexes cited above, the dihedral angles between the mean planes being 136° (**4**), 136° (**5**), and 130° (**7**). The Ru−C distances to the terminal carbon atoms of the (1−4-η)-diene fragment of **4**, **5**, and **7** (2.22−2.24 Å) are significantly greater than those to the inner carbon atoms (2.16−2.17 Å), but the difference is not so marked as in **2**.

Fluxional Behavior. Carbon-13 magnetization transfer measurements were performed on **2** at −38 °C using a selective DANTE π-pulse to invert the signal due to C^4 at δ 134.7. Figure 5 shows the ^{13}C NMR spectrum and a difference spectrum between the fully relaxed spectrum, a delay of 10 s, and an intermediate exchange spectrum, with a delay of 0.08 s between the selective DANTE pulse and the general observe pulse. There is clearly a strong transfer of magnetization from C^4 to the carbon atoms of the (1−4-η)-C_8H_8 ring, showing that ring interchange is dominant. However, there is also more exchange to C^1 than to C^2 and C^3 of the (1−6-η)-ring.[47] If the magnetization were being transferred from C^4 to C^1, C^2, and C^3 via the (1−4-η)-C_8H_8 carbon atoms, there would be equal transfer to each site. The resulting data were fitted as described previously[48] to yield a rate of exchange from one site of the (1−6-η)-C_8H_8 ring to the (1−4-η)-C_8H_8 ring of 5.7 s^{-1}, i.e., 1.4 s^{-1} for ring interchange, and a rate for 1,5-shift of the (1−6-η)-C_8H_8 ring of 0.9 s^{-1}. No evidence was found for any other fluxional process, such as a 1,3-shift of (1−6-η)-C_8H_8. The excellent agreement between experimental and calculated data is evident from Figure 6. Particularly noteworthy is the response of the signal at δ 98.3 due to C^1 (Figure 6b), which shows the more rapid transfer of magnetization to this signal due to the direct 1,5-shift. There is also a small induction period for the transfer to the signals at δ 91.3 and 78.3, owing to the transmission through the (1−4-η)-C_8H_8 ring. The derived rates correspond to free energies of activation $\Delta G^{\ddagger}_{235}$ of 12.8 ± 0.2 kcal mol^{-1} for ring interchange and 13.5 ± 0.2 kcal mol^{-1} for the 1,5-shift of the (1−6-η)-C_8H_8 ring in **2**.

The line widths of the ^{13}C signals of **4** at 2 °C in CD_2Cl_2 were determined by line-fitting as 2.0 Hz for the carbon atoms of (1,2,5,6-η)-C_8H_8, 31.5 Hz for C^3 and C^2 of (1−4-η)-C_8H_8 at δ 31.1 and 56.4, and 16.5 Hz for C^4 and C^1 at δ 117.1 and 98.0. Application of the equation $k = \pi(w - w_0)$, where w is the measured line width and w_0 is the line width in the absence of exchange (taken as 2 Hz),[49] yields the rate, k, of leaving C^3 and C^2 as 93 s^{-1} and that of leaving C^4 and C^1 as 46 s^{-1}. The fact that C^1 and C^4 broaden at half the rate of C^2 and C^3 is consistent with a 1,2-shift mechanism,[4,5] the calculated value of $\Delta G^{\ddagger}_{275}$ being 13.6 ± 0.1 kcal mol^{-1}.

This conclusion was confirmed by ^{13}C magnetization-transfer experiments in which the signals at δ 116.9 and 56.4 were separately inverted. The 1,2-shift mechanism is evident from Figures 7 and 8, which show the transfer of magnetization from C^4 at δ 116.9 successively to C^3

(46) Baenziger, N. C.; Goebel, C. V.; Berg, T.; Doyle, J. R. *Acta Crystallogr., Sect B* **1978**, *34*, 1340.

(47) A similar selective transfer of magnetization between H^1 and H^4 is also observed in the ^1H NMR spectrum, but in view of possible errors arising from the nuclear Overhauser effect, the quantitative analysis was done with the ^{13}C NMR data.

(48) Grassi, M.; Mann, B. E.; Pickup, B. T.; Spencer, C. M. *J. Magn. Reson.* **1986**, *69*, 92.

(49) Sandström, J. *Dynamic NMR Spectroscopy*; Academic: New York, 1982; p 17.

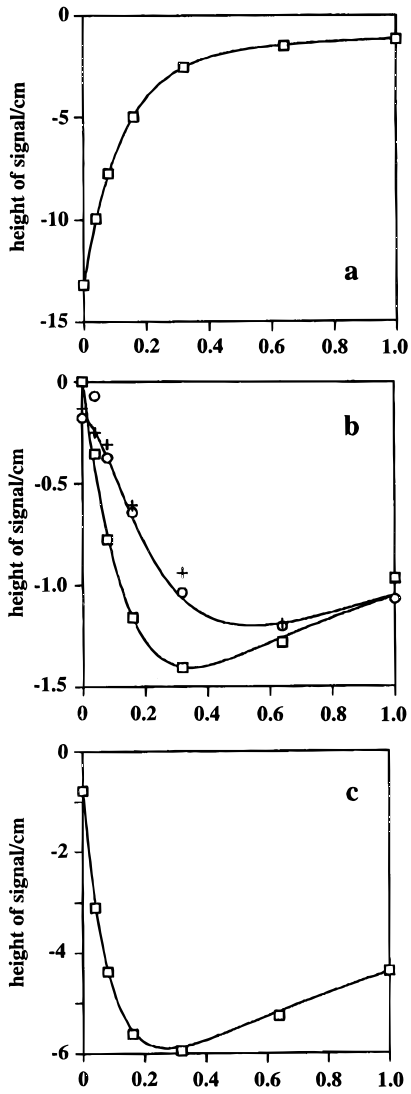

Figure 6. The changes in height of the ^{13}C NMR signals from equilibrium of [Ru((1−6-η)-C_8H_8)((1−4-η)-C_8H_8)] (**2**) after applying a selective π-pulse to the signal at δ 134.7. The times given are those between the application of the selective π-pulse and the general $\pi/2$ pulse. In each case, the symbol represents the experimental point and the continuous line the calculated fit. The noise in the spectrum is *ca.* 0.2 cm, so the fit lies within experimental error. (a) The recovery of the signal at δ 134.7, which is initially rapid as unperturbed ^{13}C nuclei exchange in from other sites and then slow as T_1 relaxation takes over. (b) The change in heights of the signals at δ 98.3 (□), 91.3 (+), and 78.3 (○). The calculated fits for the magnetization of the signals at δ 91.3 and 78.3 are so similar that only the fit for the signal at δ 91.3 is shown. (c) The change in height of the signal at δ 94.5.

at δ 130.9, C^2 at δ 56.4, and C^1 at δ 97.9. The data were fitted[50] to yield a rate for the 1,2-shift of 16.1 s^{-1} at −14 °C, corresponding to a free energy of activation $\Delta G^{\ddagger}_{259}$ of 13.7 ± 0.1 kcal mol^{-1}.

Discussion

The formation of Ru((1−6-η)-C_8H_8)((1−4-η)-C_8H_8) (**2**) from Ru(acac)$_2$((1,2,5,6-η)-C_8H_8) (**3**) and K_2[COT] builds on the work of Schrock and Lewis,[50] who first prepared carbonyl-free complexes of Ru(0) and Os(0) containing

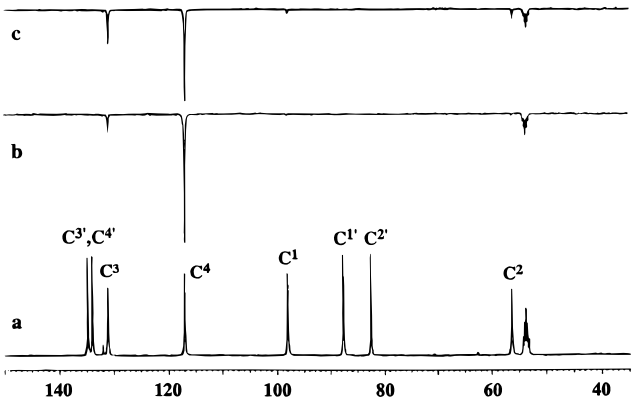

Figure 7. ^{13}C NMR spectrum at 100.62 MHz of Ru(CO)((1−4-η)-C_8H_8) ((1,2,5,6-η)-C_8H_8) (**4**) in CD_2Cl_2 at −14 °C, using the pulse sequence given in the Experimental Section. The CO resonance is not shown. The selective DANTE pulse was placed at δ 116.9. (a) Spectrum obtained with τ = 15 s. (b) Spectrum obtained by subtracting spectrum a from the spectrum obtained with τ = 0.02 s. (c) Spectrum obtained by subtracting spectrum a from the spectrum obtained with τ = 0.08 s. The peak marked with an asterisk is due to solvent.

COT, such as Ru(COT)(NBD) and Os(COT)(COD), by reaction of K_2[COT] with the appropriate diene metal halides. Complex **2** and its derivatives **4**−**8** belong to the family of mononuclear complexes, mostly of the early transition elements, that contain COT ligands of different hapticity, e.g., M((1−8-η)-C_8H_8)((1−4-η)-C_8H_8) (M = Ti,[51,52] Zr,[53−55] Hf[54−56]), M(L)((1−8-η)-C_8H_8)((1−4-η)-C_8H_8) (M = Zr, L = THF, NH_3;[51,54] M = Zr, Hf, L = CN-*t*-Bu[54]), M((1−3-η)-C_8H_8)$_2$((1−4-η)-C_8H_8),[57] M(R)((1−8-η)-C_8H_8)((1−4-η)-C_8H_8) (M = Nb, Ta),[58] and Fe((1−6-η)-C_8H_8)((1−4-η)-C_8H_8) (**1**).[6−12] In all of the examples cited, the COT rings interchange readily in solution. An interesting feature of complexes **4**−**8** is that they contain the alternative (1,2,5,6-η)- and (1−4-η)-bonding modes and that these do not interconvert rapidly on the NMR time scale. In general, the (1,2,5,6-η)-mode is found in complexes of the later transition elements in positive oxidation states, such as Pt(II), Pd(II), and Rh(I), whereas the (1−4-η)-mode is found for the early transition elements (see above) and for Fe(0) and Ru(0).[2,3] The energy difference between the two modes cannot be large because there are at least two cases, *viz.* MCp*(COT) (M = Rh, Ir), where an initially formed (1−4-η)-complex can be detected before it isomerizes to the more stable (1,2,5,6-η)-form.[59] We have no evidence for the isomerization of **4**−**8** to Ru(L)((1−4-η)-C_8H_8)$_2$, even though in the closely related compound Fe(CO)((1−4-η)-C_4H_6)((1−4-η)-C_8H_8)[60] the (1−4-η)-form of COT is

(50) Schrock, R. R.; Lewis, J. *J. Am. Chem. Soc.* **1973**, *95*, 4102.
(51) Breil, H.; Wilke, G. *Angew. Chem., Int. Ed. Engl.* **1966**, *5*, 898.
(52) Dietrich, H.; Soltwisch, M. *Angew. Chem. Int. Ed. Engl.* **1969**, *8*, 765.
(53) Kablitz, H-J.; Wilke, G. *J. Organomet. Chem.* **1973**, *51*, 241.
(54) Bemo, P.; Floriani, C.; Chiesi-Villa, A.; Rizzoli, C. *J. Chem. Soc., Dalton Trans.* **1991**, 3085.
(55) Rogers, D. M.; Wilson, S. R.; Girolami, G. S. *Organometallics* **1991**, *10*, 2419.
(56) Kablitz, H-J.; Kallweit, R.; Wilke, G. *J. Organomet. Chem.* **1972**, *44*, C49.
(57) Guggenberger, L. J.; Schrock, R. R. *J. Am. Chem. Soc.* **1975**, *97*, 6693.
(58) Schrock, R. R.; Guggenberger, L. J.; English, A. D. *J. Am. Chem. Soc.* **1976**, *98*, 903.
(59) Smith, A. K.; Maitlis, P. M. *J. Chem. Soc., Dalton Trans.* **1976**, 1773.
(60) Carbonaro, A.; Greco, A. *J. Organomet. Chem.* **1970**, *25*, 477.

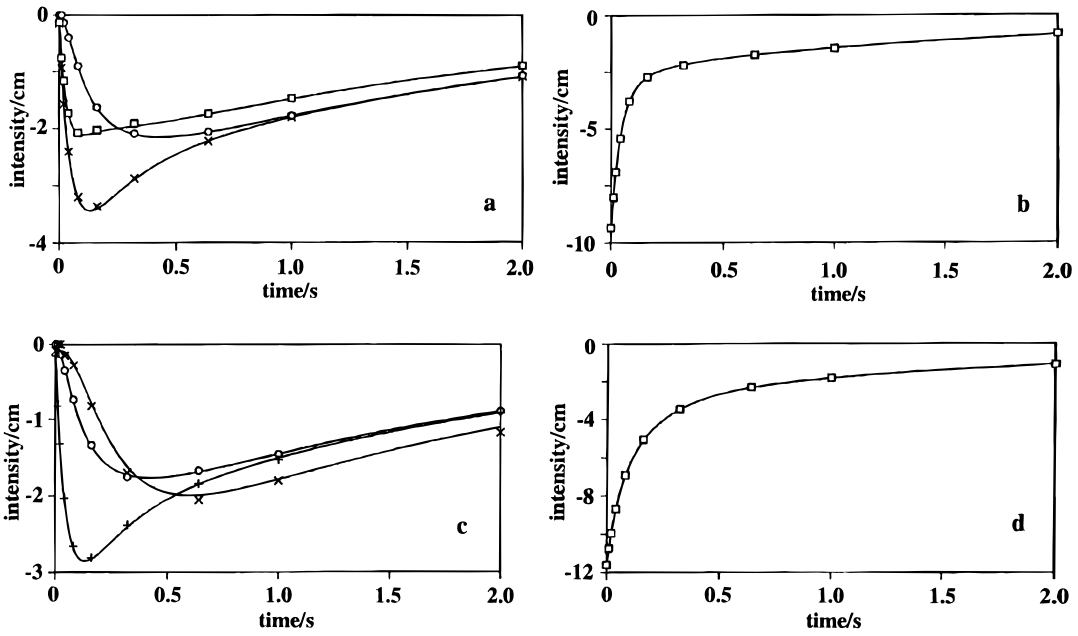

Figure 8. A plot of the magnetization of the ^{13}C NMR signals of Ru(CO)((1−4-η)-C_8H_8)((1,2,5,6-η)-C_8H_8) (**4**) in CD_2Cl_2 at −14 °C after applying a selective π-pulse. The times given are those between the application of the selective π-pulse and the general $\pi/2$-pulse. In each case, the symbol represents the experimental point and the continuous line the calculated fit. The noise in the spectrum is *ca.* 0.2 cm, so the fit lies within experimental error. (a) Changes in height of the signals at δ 130.9 (□), 116.9 (○), and 97.9 (×) on application of a π-pulse to the signal at δ 56.2. (b) Changes in height of the signal at δ 56.2 (□) on application of a π-pulse to it. (c) Changes in height of the signals at δ 130.9 (+), 97.9 (×), and 56.2 (○) on application of a π-pulse to the signal at δ 116.9. (d) Changes in height of the signal at δ 116.9 (□) on application of a π-pulse to it.

apparently favored. The (1−8-η)- to (1−4-η)-conversion observed in the early transition metal complexes presumably requires less reorganization of the COT ring than a (1−4-η)/(1,2,5,6-η)-interconversion.

The conversion of (1−6-η)-C_8H_8 in **2** to (1,2,5,6-η)-C_8H_8 in **4**-**8** by addition of two-electron donors is similar to that occurring in the formation of Mo$(CO)_4$((1,2,5,6-η)-C_8H_8) from Mo$(CO)_3$((1−6-η)-C_8H_8),[61] although the latter process is reversible. Displacement of the more weakly bound central carbon atoms of the (1−6-η)-C_8H_8 fragment of **2** by an entering ligand to give (1,2,5,6-η)-C_8H_8 can be readily envisioned. However, this behavior is not general; the reaction of Ru((1−6-η)-C_8H_8)(η^4-NBD) with group 15 donor ligands gives Ru(L)((1−4-η)-C_8H_8)-(η^4-NBD).[50,62]

As noted above, **1** and **2** adopt different rotameric configurations, which probably do not differ greatly in energy and which evidently interconvert rapidly on the NMR time scale. In the case of Os((1−6-η)-C_8H_8)(η^4-1,5-COD), two rotational processes can be observed: an oscillation with a $\Delta G^‡$ value of 8.9 kcal mol^{-1} and a complete rotation with an estimated $\Delta G^‡$ value of *ca.* 11.5 kcal mol^{-1}.[62] Since no corresponding processes were observed in Ru((1−6-η)-C_8H_8)(η^4-NBD), the barriers to ring rotations may be lower in ruthenium compounds than in their osmium analogues.

The activation barriers to the 1,2-shift in the (1−4-η)-C_8H_8 rings of **2** and **4** are remarkably different, despite the similarity of the geometry of the coordinated ring (particularly the hinge angle) in both compounds. Any line broadening in the ^1H NMR signals of **2** at −100 °C due to slowing of the fluxional process is less than 3 Hz. Assuming the ^1H chemical shifts to be similar to those of Ru$(CO)_3$((1−4-η)-C_8H_8) at −100 °C,[63] a lower limit for the rate of the process at −100 °C is 10^5 s^{-1}, corresponding to an upper limit for $\Delta G^‡$ of 6 kcal mol^{-1}. A similar estimate has been made for Ru(η^6-C_6Me_6)((1−4-η)-C_8H_8),[41] whereas the activation barriers $\Delta G^‡$ for Ru$(CO)_3$((1−4-η)-C_8H_8)[63] and Ru(CO)((1−4-η)-C_8H_8)-((1,2,5,6-η)-C_8H_8) (**4**) are 7.7 and 13.7 kcal mol^{-1}, respectively. Values of $\Delta G^‡$ for the 1,2-shift of (1−4-η)-C_8H_8 in the range 13 kcal mol^{-1} have also been reported for Ru(L)((1−4-η)-C_8H_8)(η^4-NBD) (L = PEt_3, $P(OMe)_3$).[62] The reason for the comparatively high values in these compounds and in **4** is that the 1,2-shift of the metal atom, which corresponds to a symmetry-allowed 1,5-sigmatropic shift, produces an isomer **4d** of **4**, as shown in Scheme 1. The activation energy of the process must be sufficient to twist the remaining ligands to reform **4**. A similar argument has been put forward to account for the 1,5-sigmatropic process in Fe$(CO)_2$(CN-*i*-Pr)((1−4-η)-C_8H_8),[64] and the process of ligand twisting has been observed in, for example, Ru$(CO)_{3-n}L_n$((1−4-η)-diene) (L = $P(OCH_2)_3CEt$) ($\Delta G^‡$ *ca.* 12 kcal mol^{-1}).[65] Conversely, the very low barrier to the 1,5-sigmatropic shifts in **2** and Ru(η^6-C_6Me_6)((1−4-η)-C_8H_8) may indicate that the process in these molecules is coupled with the relative rotation of the two rings.

Sigmatropic shifts in (1−6-η)-C_8H_8 rings are symmetry-forbidden; hence, the activation energies for fluxional processes are generally 5−10 kcal mol^{-1} higher than those in (1−4-η)-C_8H_8 rings.[5] For M$(CO)_3$((1−6-η)-C_8H_8) (M = Cr,W), both 1,3- and 1,2-shifts occur, the

(61) Kaesz, H. D.; Winstein, S.; Kreiter, G. *J. Am. Chem. Soc.* **1966**, *88*, 1319.
(62) Grassi, M.; Mann, B. E.; Pickup, B. T.; Spencer, C. M. *J. Chem. Soc., Dalton Trans.* **1987**, 2649.
(63) Cotton, F. A.; Hunter, D. L. *J. Am. Chem. Soc.* **1976**, *98*, 1413.
(64) Hails, M. J.; Mann, B. E.; Spencer, C. M. *J. Chem. Soc., Dalton Trans.* **1985**, 693.
(65) Whitesides, T. M.; Budnik, R. A. *Inorg. Chem.* **1975**, *14*, 664.

Scheme 1. The Symmetry-Allowed 1,5-Sigmatropic Shift Mechanism Applied to Ru(CO)((1−4-η)-C_8H_8)((1,2,5,6-η)-C_8H_8) (4)[a]

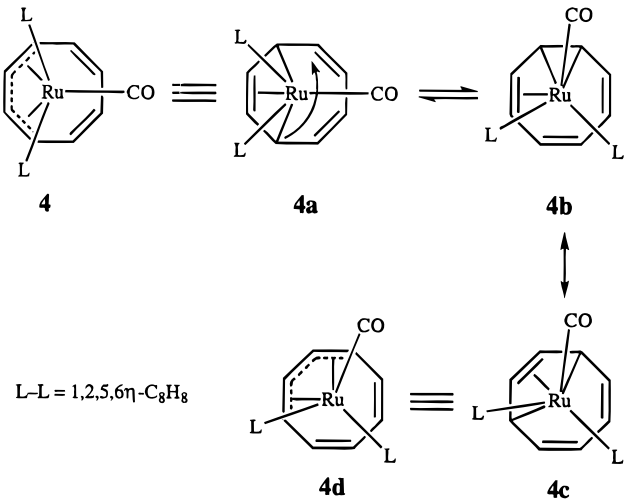

[a] The shift converts **4a**, a valence-bond representation of **4**, into **4b** with a resulting rotation of the ligands attached to ruthenium. **4c** is an alternative valence-bond representation of **4b** which is normally represented by **4d**.

former predominating,[66,67] whereas for Os((1−6-η)-C_8H_8)-(η^4-1,5-COD) and Ru((1−6-η)-C_8H_8)(η^4-NBD), both 1,5- and 1,3-shifts are observed, the former being dominant.[62] These shifts are believed to occur by displacement of one of the coordinated double bonds by the previously uncoordinated double bond. For **2**, only a 1,5-shift can be detected. In view of both the reaction of **2** with the ligands and the trends in the Ru-C((1−6-η)-C_8H_8) distances, it seems plausible that the central double bond of the (1−6-η)-C_8H_8 unit is detached and replaced by the initially uncoordinated double bond. The intermediate or transition state in such a process could be a 16-electron species, Ru((1−4-η)-C_8H_8)((1,2,5,6-η)-C_8H_8), analogous to the known four-coordinate ruthenium(0) complexes Ru(η^2-styrene)$_2$(PPh_3)$_2$[68] and Ru(CO)$_2$(P-*t*-Bu_2Me)$_2$[69] which show a distorted tetrahedral geometry. Likewise, the exchange of roles between the (1−4-η)- and (1−6-η)-rings of **2** could proceed via a 16-electron species Ru((1−4-η)-C_8H_8)$_2$. In both cases, however, an intermediate or transition state in which both the departing and entering double bonds are partially bound to the metal atom cannot be ruled out.

Acknowledgment. We thank BASF (Ludwigshafen, Germany) for a gift of cyclooctatetraene and Johnson-Matthey Co., U.K., for a loan of hydrated ruthenium(III) chloride.

Supporting Information Available: Tables of crystallographic data, atomic coordinates and isotropic displacement factors, anisotropic displacement parameters, interatomic distances involving hydrogen atoms, interatomic angles involving non-hydrogen and hydrogen atoms, torsion angles involving non-hydrogen atoms, nonbonded contacts, and selected least-squares planes and dihedral angles for **2**, **4**, **5**, and **7** and thermal ellipsoid diagrams of **4** and **5** (84 pages). Ordering information is given on any current masthead page.

OM970065J

(66) Gibson, J. A.; Mann, B. E. *J. Chem. Soc., Dalton Trans.* **1979**, 1021.
(67) Abel, E. W.; Orrell, K. G.; Qureshi, K. B.; Sik, V.; Stephenson, D. *J. Organomet. Chem.* **1988**, *353*, 337.
(68) Carrondo, M. A. A. F. de C. T.; Chaudret, B. N.; Cole-Hamilton, D. J.; Skapski, A. C.; Wilkinson, G. *J. Chem. Soc., Chem. Commun.* **1978**, 463.
(69) Ogasawara, M.; Macgregor, S. A.; Streib, W. E.; Folting, K.; Eisenstein, O.; Caulton, K. G. *J. Am. Chem. Soc.* **1995**, *117*, 8869.